Escola d'Enginyeria de Telecomunicació i Aeroespacial de Castelldefels
UNIVERSITAT POLITÈCNICA DE CATALUNYA

BACHELOR'S THESIS

TITLE: Estimation of fuel inefficiencies due to early descents

DEGREE: Bachelor's Degree in Airport Engineering

AUTHOR: David A. Lesmes-Chávez

ADVISERS: Ramon Dalmau
Xavier Prats

DATE: October 24, 2018

Title: Estimation of fuel inefficiencies due to early descents.

Author: David A. Lesmes-Chávez

Advisers: Ramon Dalmau
Xavier Prats

Date: October 24, 2018

Abstract

In this project, early descents have been modeled as a combination of two stages. Firstly, a constant-vertical-speed segment beginning at a certain distance, *k*, before the optimal top of descent (TOD); that eventually intercepts the second stage: a nominal (ideal) continuous descent trajectory that would have begun at the optimal TOD and would have then descended at idle thrust until reaching FL100. In both cases, an optimal Mach/CAS profile is maintained.

The aforementioned two stages have been simulated separately for several mass (*m*), cruise altitude (*z*) and cost index (*CI*) values using AIRBUS' Performance Engineering Programs (PEP). In the proposed model, these two trajectories begin at the same point with the same input settings. However, they do not start descending at the same time, with the TOD of the second stage laying a *k* distance away from the TOD of the first. For this reason, an initial *k* distance cruise segment has been added to the second stage when simulating.

The fuel consumption of both cases was analyzed and compared using custom Python scripts in order to get a preliminary understanding of the sensitivity of fuel consumption to the independent variables; and to check for identifiable patterns. Fuel inefficiency was thus defined as the extra fuel consumption resulting from anticipating descent initialization, and calculated as the difference in aircraft mass (*m*) between the TOD of the first stage and the point in which the constant-vertical-speed trajectory intercepts the idle-thrust type.

For the aircraft used in this study, the A320-232, the extra fuel consumption incurred by an early descent reached a maximum relative value of 22.63% and a maximum absolute value of 116.9 kg (when *k* = 75 NM); showing the importance of further research into this topic.

Títol: Estimació d'ineficiències en combustible degudes a descensos anticipats.

Autor: David A. Lesmes-Chávez

Directors: Ramon Dalmau i Codina
Xavier Prats i Menéndez

Data: 24 d'octubre de 2018

Resum

En aquest projecte, s'han modelat els descensos anticipats com la combinació de dues etapes. En primer lloc, un segment a velocitat vertical constant que comença a una certa distància, k, del punt d'inici del descens (*TOD, top of descent*) òptim; que posteriorment intercepta la segona etapa: una trajectòria de descens nominal (ideal) continu que hagués començat al TOD òptim i que després hagués descendit amb empenta en punt mort fins a arribar a FL100. En tots dos casos, es manté un perfil òptim de Mach i velocitat calibrada (*CAS, calibrated airspeed*).

Cadascuna de les dues etapes precitades ha estat simulada per separat al software PEP (Performance Engineering Programs) de AIRBUS; emprant diversos valors de massa (*m*), altitud de creuer (*z*) i índex de cost (*CI, cost index*). Al model proposat, aquestes dues trajectòries comencen al mateix punt i amb les mateixes configuracions inicials. Tanmateix, no es comença el descens simultàniament, atès que el TOD de la segona etapa es troba a una distància k del TOD de la primera. Per aquesta raó, en simular la segona etapa se li ha afegit un segment inicial de creuer de distància k.

El consum de combustible d'ambdós casos es va analitzar i comparar utilitzant scripts de Python propis, per tal d'assolir una comprensió preliminar de la sensibilitat del consum de combustible als efectes de les variables independents; i també, per intentar identificar patrons. La ineficiència en combustible va ser doncs definida com el consum addicional de combustible que resulta d'haver anticipat la inicialització del descens, i calculada com la diferència en massa (*m*) de l'aeronau entre el TOD de la primera etapa i el punt en el qual la trajectòria a velocitat vertical constant intercepta aquella d'empenta en punt mort.

Per l'aeronau utilitzada en aquest estudi, la A320-232, el consum addicional de combustible degut a un descens anticipat va arribar a un valor màxim relatiu de 22.63% i a un valor màxim absolut de 116.9 kg (quan k = 75 NM); demostrant la importància de promoure la recerca sobre aquest tema.

Título: Estimación de ineficiencias de combustible debidas a descensos anticipados.

Autor: David A. Lesmes-Chávez

Directores: Ramon Dalmau
Xavier Prats

Fecha: 24 de octubre de 2018

Resumen

En el presente proyecto, los descensos anticipados se han modelado como la combinación de dos etapas. En primer lugar, un segmento a velocidad vertical constante que comienza a una cierta distancia, *k*, antes del punto de inicio del descenso (TOD, *top of descent*); y que eventualmente intercepta una segunda etapa: una trayectoria nominal (ideal) continua que hubiese empezado en el TOD óptimo y que luego hubiese descendido con empuje en ralentí hasta alcanzar FL100. En los dos casos se mantiene un perfil óptimo de Mach y velocidad calibrada (CAS, *calibrated airspeed*).

Ambas etapas se han simulado por separado con diferentes valores de masa (*m*), altitud de crucero (*z*) e índice de coste (*CI, cost index*), utilizando el software PEP (*Performance Engineering Programs*), creado por Airbus. En el modelo propuesto, estas dos trayectorias inician en el mismo punto con idénticas configuraciones iniciales. No obstante, el descenso no se inicia simultáneamente, ya que el TOD de la segunda etapa se halla a una distancia *k* del TOD de la primera. En consecuencia, a la hora de simular se le ha añadido a la segunda etapa, un segmento de crucero inicial de distancia *k*.

El consumo de combustible de ambos casos ha sido analizado y comparado usando scripts de Python propios, con el propósito de esbozar una comprensión preliminar de la sensibilidad del consumo de combustible a los efectos de las variables independientes; intentando identificar posibles patrones. Por su parte, la ineficiencia de combustible fue definida como el consumo extra de combustible que resulta de haber anticipado el inicio del descenso; y calculada como la diferencia en masa del avión (*m*) entre el TOD de la primera etapa y el punto en el cual la trayectoria a velocidad vertical constante intercepta aquella del empuje en ralentí.

Para la aeronave del estudio, el A320-232, el consumo extra de combustible debido a un descenso anticipado alcanzó un valor máximo relativo de 22.63% y un valor máximo absoluto de 116.9 kg (para *k* = 75 NM); mostrando la importancia de profundizar la investigación en este tema.

Título: Estimação de ineficiências de combustível devidas a descensos antecipados.

Autor: David A. Lesmes-Chávez

Orientadores: Ramon Dalmau
Xavier Prats

Data: 24 de outubro de 2018

Resumo

No presente projeto, as descidas antecipadas foram modeladas como uma combinação de duas etapas. Em primeiro lugar, um segmento de velocidade vertical constante começando a uma certa distância, *k*, antes do topo da descida (TOD) ótimo; que posteriormente intercepta uma segunda etapa: uma trajetória de descida nominal (ideal) continua que tivesse começado no TOD ótimo e que depois tivesse descido com empuxo em *ralenti* até o FL100. Nos dois casos mantém-se um perfil ótimo de Mach e velocidade calibrada (*CAS, calibrated airspeed*).

As duas etapas foram simuladas por separado com diferentes valores de massa (m), altitude de cruzeiro (*z*) e índice de custo (CI, *cost index*), usando o software PEP (*Performance Engineering Programs*) da Airbus. No modelo proposto, as duas trajetórias iniciam no mesmo ponto com idênticas configurações iniciais. Porém, a descida não começa de maneira simultânea porquanto o TOD da segunda etapa acha-se a uma distância *k* do TOD da primeira. Por conseguinte, no momento de fazer as simulações, adicionou-se à segunda etapa um segmento de cruzeiro inicial de distância *k*.

O consumo de combustível de ambos casos foi analisado e comparado com scripts de Python próprios, a fim de obter uma compreensão preliminar da sensibilidade do consumo de combustível às variáveis independentes; tentando identificar possíveis patrões. Por sua vez, a ineficiência de combustível foi definida como o consumo adicional de combustível resultante da antecipação da inicialização da descida; e calculada como a diferença em massa do avião (*m*) entre o TOD da primeira etapa e o ponto no qual a trajetória de velocidade vertical constante intercepta aquela do empuxo em *ralenti*.

Para a aeronave do estudo, o A320-232, o consumo adicional de combustível devido a uma descida antecipada atingiu um valor máximo relativo de 22,63% e um valor máximo absoluto de 116,9 kg (para k = 75 NM); mostrando a importância de aprofundar na pesquisa sobre o tema.

Hïká: «*Ästimäsÿó tz'inäfisÿénsÿäs tze kumpzustíblä tzägútzäs a tzäsénsus äntisipasx*» (Kätälkubzun bihistaká).

Kiska: Tzakzo Suagwá-Lesmes.

Asaná cxiska: Rzämón Tzälmáw ngá Šäfzÿé Prasx.

Zokam 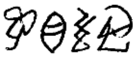, **cié** amubcihikán cxona, **swá** wetas asák mïhïkán.

Hyca: Hÿašúakïk-ïnšié kïkawacxonúka mïsá.
Šis: cxïpkïkïnšié.

[illegible]

Ուշ Լինի, Անուշ Լինի…

Gràcies, Ramon, per la idea original d'aquest TFG, per salvar-me en un vespre de programació i llegir-te, paraula per paraula les diferents versions que ha tingut aquest treball.

Gràcies, Xevi, per les correccions sense les quals aquest document no es veuria com es veu ara. També pel temps extra per fer aquest document molt meu.

Gràcies, Yolanda, perquè en un país on l'educació pública costa, la teva perseverança ha fet possible tancar el finançament d'aquest treball.

Gràcies, Mercè, Txus, Mar, Teresa, Núria, Glòria, Laia, Montse, Mayra i Mayte per estar tan pendents de com anava tot; per donar-me ànims quan no ho veia gens clar; i per confiar en mi més del que jo mateix confio. I pels riures, clar... Al CBL només es pot sobreviure rient.

Gràcies, Clàudia per ser el meu Google de TFG personalitzat; i junt amb la Kika, motivadores number one. Com no us heu cansat de les meves queixes... no ho entendré pas mai.

Gràcies, BEST Barcelona, i el poble de Cantuslunya. Amb tots vosaltres m'he "developejat" com no ho hagués pensat mai; i gràcies a vosaltres he arribat tan lluny com volia. Aquest remix del Dago Yankee també va per vosaltres.
Uni ex, Vita laboralis in.

Gràcies, Víctor, Laura i Àngels per acollir-me en tots els sentits possibles.

Gracias, Pilar, por haber mantenido la puerta de tu despacho siempre abierta. De antemano me excuso por la total ausencia de tortugas en este documento.

Gracias, Gus, por ser el mejor padre putativo posible. No hace falta que me eches vino encima esta vez.

Gracias... Ángela M Beltrán Hernández; por *tanto*. Haces falta.

Vielen Dank Nicole, für deine Unterstützung und deine guten Wünsche. Madonna! ~~zieh dir~~ Bitte ~~etwas an~~ sag mir, dass du es auch geschafft hast deine Abschlussarbeit zu beenden.

Спасибо, мои русские жёны, за вашу любовь, за ваши души.
И тебя, Элечка, люблю тебя до Тамбова и обратно.

Merci, Charlie, pour être mon frère officiel. Après Rio et Montréal... la troisième fois sera-t-elle la bonne ?

Canım, bu senin (ve köpeklerimiz) için: unutma!
Ben unutmayacağım...

E hoʻomau i ko kāua aloha, kau ā kau.

“Dann somin pavé na avansé,
Sa pa malizé pou nou kapoté.

Na ankor pour éspéré
Si somin nou mèm la galizé.”

“On beaten paths we shall forge on,
No ill winds can sway or topple us.

There are still things to hope for
On paths we’ve cleared ourselves.”

CONTENTS

LIST OF FIGURES

LIST OF TABLES

ACRONYMS AND ABBREVIATIONS

AP/FD	Autopilot (Flight Director)
A/THR	Autothrottle
ATC	Air Traffic Control
ATCO	Air Traffic Controller Officer
ATM	Air Traffic Management
CAS	Calibrated Airspeed
CDO	Continuous Descent Operations
FAA	Federal Aviation Administration
FCOM	Flight Crew Operating Manual
FCU	Flight Control Unit
FL	Flight Level
FMGS	Flight Management and Guidance System
FMS	Flight Management System
IAF	Initial Approach Fix
IATA	International Air Transport Association
ICAO	International Civil Aviation Organization
KCAS	Calibrated Airspeed (in knots)
MLW	Maximum Landing Weight
MTOW	Maximum Take-Off Weight
MMO	Maximum Operating Mach
PEP	Performance Engineering Programs
TMA	Terminal Maneuvering Area
TOD	Top Of Descent
V/S	Vertical Speed
VMO	Maximum Operating Speed

NOMENCLATURE

$CAS_{descent}$	Calibrated airspeed used in a calculated descent profile
CI	Cost index
f	Fuel consumption (as defined in 2.1.1.)
f_b	Fuel consumption of a baseline trajectory
f_k	Fuel consumption of a comparative trajectory
h	Altitude at which a constant-vertical-speed descent trajectory meets an idle-thrust descent one (also referred to as interception point).
k	Distance between TOD_{idle} and TOD_{vs}
m	Mass
$M_{descent}$	Mach number used in a calculated descent profile
TOD_{idle}	Top of descent of an idle-thrust descent trajectory
TOD_{vs}	Top of descent of a constant-vertical-speed descent trajectory
z	Cruise altitude at which a descent trajectory has begun
α^*	Fuel inefficiency

INTRODUCTION

Worldwide, the Air Traffic Management (ATM) system is currently moving from a rather static airspace-based paradigm to a more dynamic trajectory-based one. Placing the spotlight on individual aircraft has unearthed a new dimension of issues and related research. And with constantly increasing air traffic, even the smallest details of flight planning and execution are being examined. This has, in turn, highlighted the need for further optimization of all phases in a flight. Several variables can be the object of this optimization: time, several different costs, noise, fuel, etc.; and ***fuel efficiency*** is one of the most commonly discussed topics in the field currently, because it represents both economic and environmental benefits (not only for the aircraft operator, but for the system as a whole).

The concept of Continuous Descent Operations (CDO) was proposed as a way to increase fuel efficiency during the flight phase known as ***descent*** (the one that closes the cruise phase and prepares the aircraft for its final approach). It has already been demonstrated that CDO are successful in the reduction of noise nuisance, emissions and fuel consumption in the Terminal Maneuvering Area (TMA) [1]. And in order to reap the maximum benefits of CDO, aircraft should descend with idle engines from its optimal ***top of descent (TOD)***.

Accordingly, CDO procedures have been analyzed by several authors; with most of them using energy as the independent variable and aiming for energy-neutral trajectories[1]. Particularly, Park and Clarke [2] have investigated fuel consumption in CDO optimal procedures (with their model including a differentiated descent segment from the TOD to 10 000 ft). The same differentiated descent segment was included by Dalmau and Prats [3] when studying controlled time of arrival windows in certain CDO.

However, these studies tend to include CDO trajectories in which the TOD is optimal. The optimal TOD is calculated by the Flight Management System (FMS) along with the optimal descent trajectory; but the compliance with it is not the responsibility of the FMS itself: pilots are the ones who must initiate descent at the optimal TOD after getting clearance from Air Traffic Control (ATC).

In a "*descend when ready*" clearance (issued before the optimal TOD) pilots are free to follow the optimal descent trajectory, whereas a constrained descent clearance will cause alterations. Sometimes, even if the pilot can comfortably reach the optimal TOD, they might opt not to (owing to operators' preferences, the need for a repressurization segment, or other factors). In any of the previous cases, it is possible that the pilot starts the descent before the optimal TOD, generating an ***early descent*** (during such, guidance strategies embedded in typical FMSs aim at intercepting the optimal descent trajectory planned at idle thrust from below by maintaining a shallower constant vertical speed with the elevator and by following the original speed profile with the auto-throttle).

[1] These trajectories are such that they can be adjusted without requiring additional thrust nor speed-brakes, by exchanging "altitude for airspeed (and vice versa) to gain or lose time and energy through elevator control" [3].

By the time of this thesis' writing, no other work had specifically assessed fuel inefficiencies produced by said type of descent. This is why in this project a simplified model has been devised to test the effect of the TOD anticipation's distance (named *k* throughout this work) in fuel consumption (using different mass (*m*), cruise altitude (*z*) and cost index (*CI*) values for a model aircraft).

The first chapter introduces the basic definitions and values behind: the selected model aircraft; descent as a flight phase (and how it is planned and executed by the FMS of the selected aircraft, plus, a brief section on the involvement of ATC); and the PEP software.

The second chapter explains and justifies the model of the experiment and the independent variables selected, and briefly describes how data was retrieved and processed in order to get the results outlined in the third chapter. These results, in the form of plots, are discussed in the end of the third chapter and are the source of the conclusions of the project; which satisfactorily confirm that by eliminating TOD anticipation, extra fuel consumption can be avoided for certain flight conditions.

CHAPTER 1. Background

The aim of this chapter is to introduce the basic concepts, definitions and numbers behind the object of this study: the quantification of the fuel inefficiencies caused by early descents in an Airbus A320 aircraft. A short introduction of the main simulation software used is also provided in this chapter.

1.1. Airbus A320-232.

The Airbus A320 is a family of narrow-body commercial[2] passenger twin-engine jet aircraft manufactured by Airbus. As of 30 September 2018, there are 8 046 aircraft of this family in operation; and out of these, 4 353 follow the A320-ceo (Current Engine Option) model [4]. This means that the A320-ceo accounts for approximately 20.59%[3] of the planes flying nowadays.

Fig 1.1 Airbus A320-ceo [5].

The relevance of such model has prompted the author to choose it as the object of this study, more specifically the aircraft labeled by the International Aircraft Categorization and Identification Standard (IACIS) as[4]:

- Master model (basic airplane design) = A320.
- Model = A320.
- Master series (basic version of the type) = A320-200.
- Series (specific configuration by engine) = A320-232[5].

Not only is this aircraft one of the available options in the simulation software of the study; it is also commonplace in the Barcelona-El Prat Airport, where for

[2] Cargo models for the A320, the A320P2F and A321P2F have been proposed as future developments [6].
[3] Considering the current (as of 30 September 2018) number of commercial passenger jets in service as 21 145, estimated from [7].
[4] Using the taxonomy categories defined by [8]. In the European context, these taxonomy categories are usually named (from top to bottom): type, type variant, series and model [9].
[5] The fifth digit of the name of Airbus aircraft corresponds to the engine manufacturer [10].

example, the main airline by market share [11], Vueling, is estimated to own thirty-eight (38) such aircraft (out of a fleet of 113 aircraft[6], 36.6%).

This aircraft was certified in Europe by the Joint Airworthiness Authority (JAA)[7] on 28 September 1993, as the A320-200 series with a V2527-A5 engine. Among the information found in its certification document [12], some values are essential to this project:

CONCERNING MASS:

- Maximum Certified Masses:
    - Maximum Landing Weight (MLW): 64 500 kg (variants 000-003, 005, 007-010, 013-015, 019) or 66 000 kg (variants 011, 012, 016-018).
    - Maximum Take-Off Weight (MTOW): 67 000 kg (variant 005), 68 000 kg (variant 001), 70 000 kg (variants 002, 019), 71 500 kg (variants 013, 018), 73 500 kg (variants 000, 008, 014, 016), 75 500 kg (variants 003, 009, 011), 77 000 kg (variants 007, 010, 012) or 78 000 kg (variants 015, 017).

CONCERNING SPEED:

- MMO (Maximum Operating Mach): 0.82
- VMO (Maximum Operating Speed): 350 KCAS

CONCERNING ALTITUDE:

- Maximum Operating Altitude: 39 100 ft (pressure altitude)

1.2. Descent

1.2.1. General Definition

The flight phases related to the operation of a powered fixed-wing aircraft can be defined in several ways. The two most widely used taxonomies have been proposed by the International Civil Aviation Organization (ICAO) and the International Air Transport Association (IATA); and although originally used for the purpose of accident analysis, these have spread to the general research domain.

In this study, the definition of descent by the IATA is used: *"this phase begins when the crew departs the cruise altitude for the purpose of an approach at a particular destination; it ends when the crew initiates changes in aircraft configuration and/or speeds to facilitate a landing on a particular runway"* [13]. In a flight in normal conditions, this descent (DST) phase follows cruise (CRZ) and precedes approach (APR).

[6] The fleet of Vueling includes a total of ninety-two (92) A320-200 aircraft.
[7] The predecessor of the European Aviation Safety Agency (EASA).

1.2.2. Nominal Descent

A nominal (ideal) descent without altitude constraints involves three distinct stages (see Fig. 1.2) whose profile is calculated by the FMS (which aims for the optimal profile). Firstly, a constant Mach segment (ideally with idle thrust) from the top of descent (TOD) to the interception of the optimal CAS[8]; secondly, a constant CAS segment (ideally with idle thrust too) from the cross-over altitude to FL100; and lastly, a very quick (and therefore, short) idle-thrust deceleration phase at FL100 until reaching 250 kt. When the aircraft reaches 250 kt at FL100, it heads towards the Initial Approach Fix (IAF) beginning the approach phase.

It should be noted that the third stage may as well begin before reaching FL100; it ultimately depends on the FMS (for example, it can be done at constant energy share factor). The deceleration itself and what happens after it have been excluded from this study as they go out of the scope of the proposed model. A possible repressurization segment (with a default vertical speed of -350 ft/min) which can happen right after the TOD has also been disregarded.

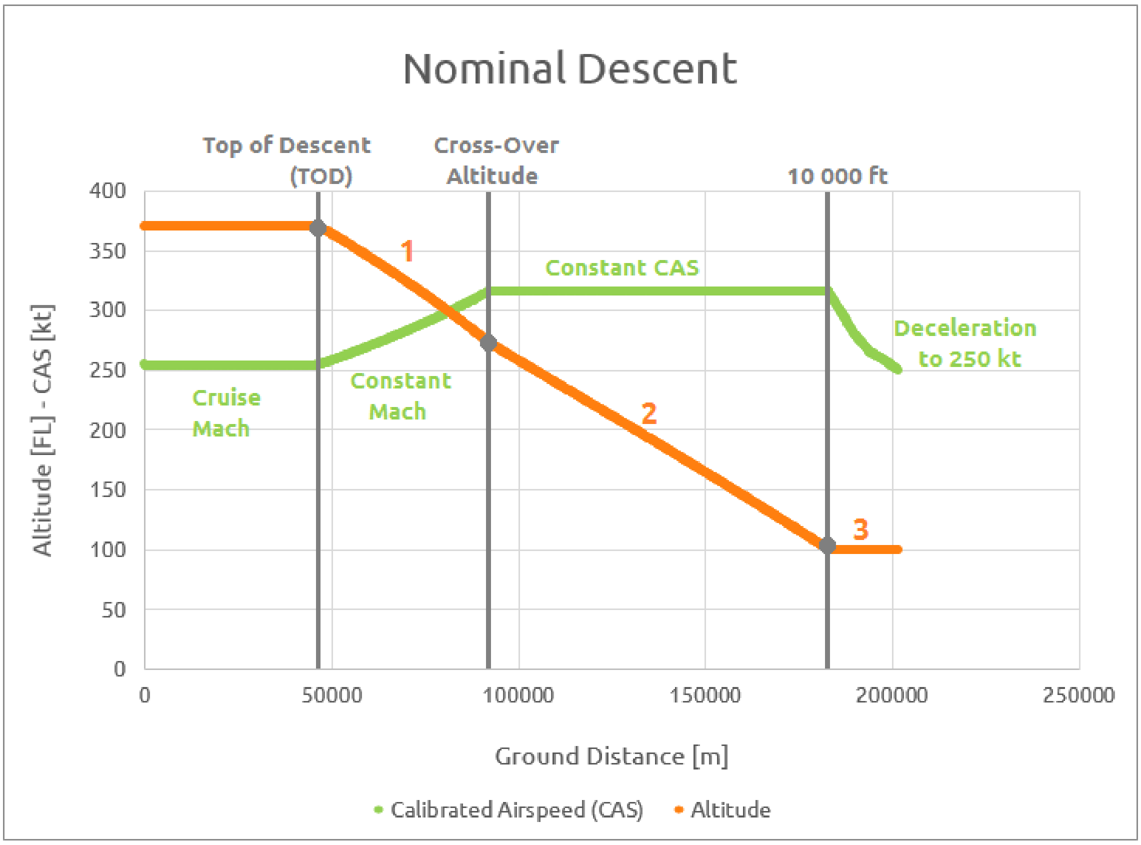

Fig. 1.2 Diagram of a nominal descent.

It is worth noting that the position of the TOD depends on the aircraft's mass (m), cruise altitude (z), distance to the destination, and optimal Mach and CAS values. These latter two are the result of minimizing a cost function that combines time

[8] The altitude at which this interception happens is called "cross-over altitude".

costs and fuel costs; therefore, they depend on the selected cost index (*CI*) (see section 2.1.2.3.), cruise altitude (*z*), desired landing mass and weather forecast. They are also limited by MMO and VMO, respectively:

$$M_{descent} \le MMO \quad \textbf{(1.1)}$$

$$CAS_{descent} \le VMO \quad \textbf{(1.2)}$$

This vertical flight profile is computed by the FMS by backwards integration from the "*Decel*" point[9]; taking into account data from the vertical and lateral flight plans, as well as wind data and any existing constraints. The aircraft may deviate from this path if: the lateral flight plan is modified, the lateral flight plan is modified, anti-icing is turned on[10], or unexpected wind conditions are encountered. This is the reason why anti-icing will be assumed as off in the proposed experiment.

1.2.3. Early Descent

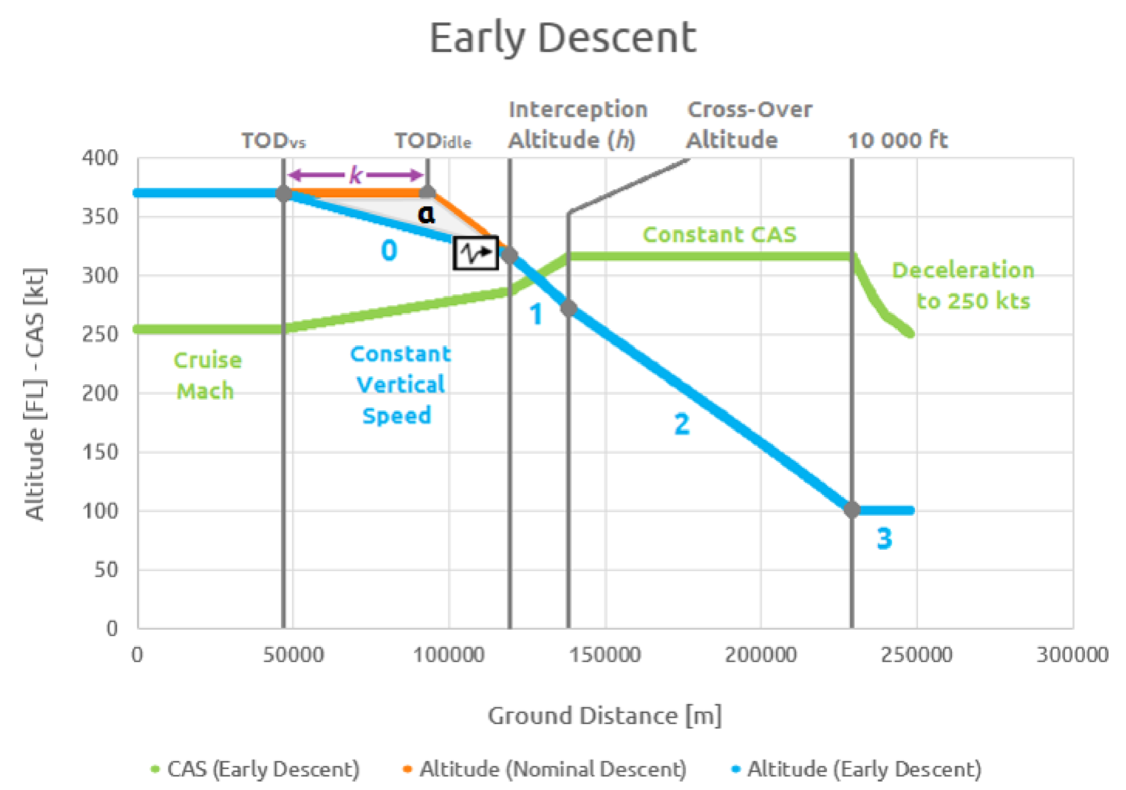

The triangle marked with an **a**, represents fuel inefficiencies.

Fig. 1.3 Diagram of an early descent.

[9] The "Decel" point is the point of the flight plan where the aircraft is predicted to decelerate in order to start its approach procedure. Its aim is to reach final approach speed (VAPP) at 1 000 ft above touchdown.
[10] Engine anti-icing is on during a descent in icing conditions: when the TAT (in flight) is at or below 10°C, and there is visible moisture in the air (such as clouds, fog with low visibility of one mile or less, rain, snow, sleet or ice crystals).

An early descent happens when descent begins not at the optimal TOD but before that, and although this is usually the result of an ATC requirement (it is even marked as such in the Flight Crew Operating Manual), it is not necessarily so.

When it occurs, the FMS acknowledges that the flight is below the optimum descent profile (see 1.2.2.) and *"maintains V/S = - 1 000 ft/min and target speed, until it reaches [a] constraint altitude or intercepts the profile*[11] *"* [14] (such interception altitude will be called *h* in this study). In order to sustain those target speeds, the elevator (controlled by the autopilot) acts to guarantee a constant vertical speed while the autothrottle acts to guarantee the target Mach or CAS. This means the throttle is pushed to a non-zero value, incurring fuel inefficiencies.

An early descent will therefore comprise up to four stages: the constant-vertical-speed one from TOD_{VS} until the interception altitude *h*; and the stages of a nominal descent starting after the interception, which might happen after the cross-over altitude (compare with Fig. 1.2). Fuel inefficiency happens when the early descent path is deviating from the ideal profile, as shown in the light grey area α of Fig. 1.3.

Table 1.1. Autothrottle and autopilot operational modes during descent [14], [15].

Stage of Descent	OPERATIONAL MODES	
	Autothrottle (A/THR)	**Autopilot Flight Director (AP/FD)**
0 (constant-vertical-speed segment)	SPEED/MACH	V/S
1 (constant Mach idle-thrust segment)	THR DES	SPEED/MACH
2 (constant CAS idle-thrust segment)	THR DES	SPEED/MACH

The autothrottle and the autopilot work in coordination to guide the aircraft: whenever one is flying a target speed, the other has to be managing a different parameter (as visible in the above table). In a constant-vertical-speed segment, the autopilot is controlling trajectory through a set vertical speed, which means that the target Mach/CAS are managed by the autothrottle. For the other two stages, speed is managed from the autopilot, which uses the elevator to change pitch attitude. Autothrottle must then be managing thrust, which it does, in THR DES (an operational mode in which thrust is kept idle).

[11] It is worth stating that an aircraft is considered to be on the vertical profile when it is within 50 feet of it [16].

1.2.4. ATC involvement

Two important reasons behind ATC-induced early descents are: on one hand, the fact that Air Traffic Control Officers (ATCOs) do not know the exact optimal TOD calculated by an aircraft's plane's FMS; and on the other, the fact that their focus is on their own workload and the safety of the arriving traffic flow rather than a single airplane's fuel consumption.

Any descent profile is thus influenced by the capacity of ATC systems and their specific requirements and constraints regarding speed, altitude and separation; especially for high traffic areas. It is worth remembering that each route is handled differently by ATCOs, according to local operational procedures and constraints established in the letter of agreements for flight transferences between different ATC entities. All of this, so as to respect the main ATC goal of allowing a shared, safe and efficient use of the airspace.

Descent cannot begin without an ATC clearance, whether given out by the ATCOs themselves or requested by the pilots. In the former case, ATC clearances may ultimately come from a set of patterns present in a specific ATC environment [17], from automated ATM systems and/or from ATCOs themselves; whose screens handle temporal, spatial and operational information related to every aircraft in their area (due to the spatiotemporal interdependencies among trajectories), usually coming from radar information. This data is useful to know whether flights are adhering to their allowed plan profiles, and if there are any infringements of the applicable separation rules (in which case these would be eliminated with special ATC clearances). Having such precise control over the descent of an aircraft (through speed and path vectors and clearances, level offs, etc.) allows for a better management of airspace [18].

From the point of view of ATC, all calculations and resulting clearances are done so as to integrate the subject aircraft into the general flow of traffic [12]. Nevertheless, flight crew faces several limitations in enacting and complying with these clearances: whether there is enough time from the point of receipt of the clearance to the point in which it must be acted upon; the current meteorological situation; the comfort of the passengers; or how to comply with the available tools and resources [19].

As it can be deducted by now, the ideal and simplified descent profile presented throughout this study is not exactly the reality of current operations. It is in fact, *"a key challenge for ATC because of the complexity and time pressure of many different types of aircraft converging on a limited landing space at an airport"* [20].

[12] Sequencing buffers help ensure safe separation among aircraft [3].

1.3. Performance Engineers' Programs (PEP)

The AIRBUS Performance Engineers' Programs (PEP) [13] package is an environment that offers several tools devoted to aircraft performance calculation within a single framework [21]. It includes three (3) low speed performance programs, four (4) high speed performance programs and two (2) additional components. For this study, two programs will be used:

- **Operational Flight Plan (OFP) =** a low speed performance program devoted to operational flight path calculation at take-off or on approach. It does calculations with OCTOPER [14], and produces text and graphical outputs. It was designed to compute operational flight paths in a three-dimensional space with its associated performance parameters, reflecting the actual aircraft capabilities under given conditions. Its "from any flight point" mode will be used.

- **In-Flight Performance (IFP) =** a high speed performance program that allows instantaneous in-flight performance data on a period of time to be computed. Each flight phase may be studied as a function of many conditions. Its "standard with FMS1 speeds" mode will be used.

[13] Airbus' PEP software provides a high degree of precision in the certified aircraft performance data and uses specific Flight Management System (FMS) algorithms for the computations.
[14] A tool whose design is based on Airbus' OCTOPUS (Operational and Certified Take-Off and landing Performance Universal Software) software, written in the form of Fortran 95 source code [22].

CHAPTER 2. Experiment

2.1. Model

This section will explain the model created to conduct the objective experiment: going first over the philosophy behind it; and then explaining the independent variables one by one and the reason behind their chosen values.

2.1.1. Overview

The model of this study aims to calculate the fuel inefficiencies induced by early descent operations by comparing two types of trajectories. On one hand, the ideal descent, which is performed with idle engines and the elevator executing the planned path while managing the speed deviation within certain bounds. On the other hand, the way most early descents work: descending with a constant vertical speed of -1 000 ft/min, controlled by the autothrottle (thus, with a variable non-zero thrust), and following the original Mach/CAS profile with the elevator until intercepting the optimal idle-thrust profile from below. In this study, the latter type will be called a ***baseline trajectory***. Anything happening after FL100 has been reached will be disregarded.

The idea behind this experiment is to have both types of trajectories meet at some point before reaching FL100, and to assume that when they meet, the baseline trajectory switches over to the ideal path. In this approach, fuel inefficiency happens when the flight is following the baseline trajectory before being able to follow the ideal one: allegedly, the faster a flight can leave the baseline trajectory, the less inefficient it will be. In order to test this hypothesis, different "meeting" altitudes should be tested (each one of these will be labeled as an h altitude). This translates to having early descents at distinct distances from the optimal TOD.

For the sake of simplicity in calculations and data handling, in this study the model will not work in the most intuitive way: each ***scenario*** will consist of one baseline trajectory (beginning at its top of descent, TOD_{VS}) and some ideal ***comparative trajectories***. These comparative trajectories will begin descending at different top of descent points (TOD_{idle}), separated a certain k distance from TOD_{VS}. This will, in practice, emulate different early descent trajectories.

For every baseline trajectory, there will be a corresponding group of up to four comparative trajectories (one for each non-zero k value). Those five simulations start at TOD_{VS} with equal mass (m), equal cruise altitude (z) and the same optimal descent Mach/CAS speed profile corresponding to a certain cost index (CI). It is their behavior afterwards what is somewhat independent for each, as shown in Fig. 2.1.

The altitude profile of the baseline trajectory is a (straight, when plotted using time as the independent variable) descending line, as it involves a constant vertical speed (-1 000 ft/min). Contrarily, comparative trajectories have three distinct phases: a cruise segment from TOD_{VS} to TOD_{idle}, an idle-thrust descent segment with constant Mach number and a final idle-thrust descent segment with constant CAS (hence the three different slopes in Fig. 2.1). It is worth noting that although poorly visible in the figure, the two last segments are not exactly the same for the comparative trajectories, given the fact that they have different masses by the end of their cruise segment.

Fuel consumption (Formula 2.1) will thus be calculated as the difference in mass between TOD_{VS} and the *h* altitude; whereas fuel inefficiency (Formula 2.2) will be calculated as the difference between the fuel consumption of the baseline trajectory and that of the comparative trajectory being evaluated; divided by the fuel consumption of that same comparative trajectory; and multiplied by a hundred (to create a percentage).

$$f = m(TOD_{VS}) - m(h) \quad \textbf{(2.1)}$$

$$\alpha^* = 100 \cdot ((f_b - f_k)/f_k) \quad \textbf{(2.2)}$$

In order to achieve the objectives of this project while keeping a reasonable scope of assessment, up to two hundred and fifty-six (256) comparative trajectories plus sixty-four (64) baseline trajectories will be created and compared. The first group corresponds to the combination of: four cruise altitudes, four masses, four cost index values and four *k* distances.

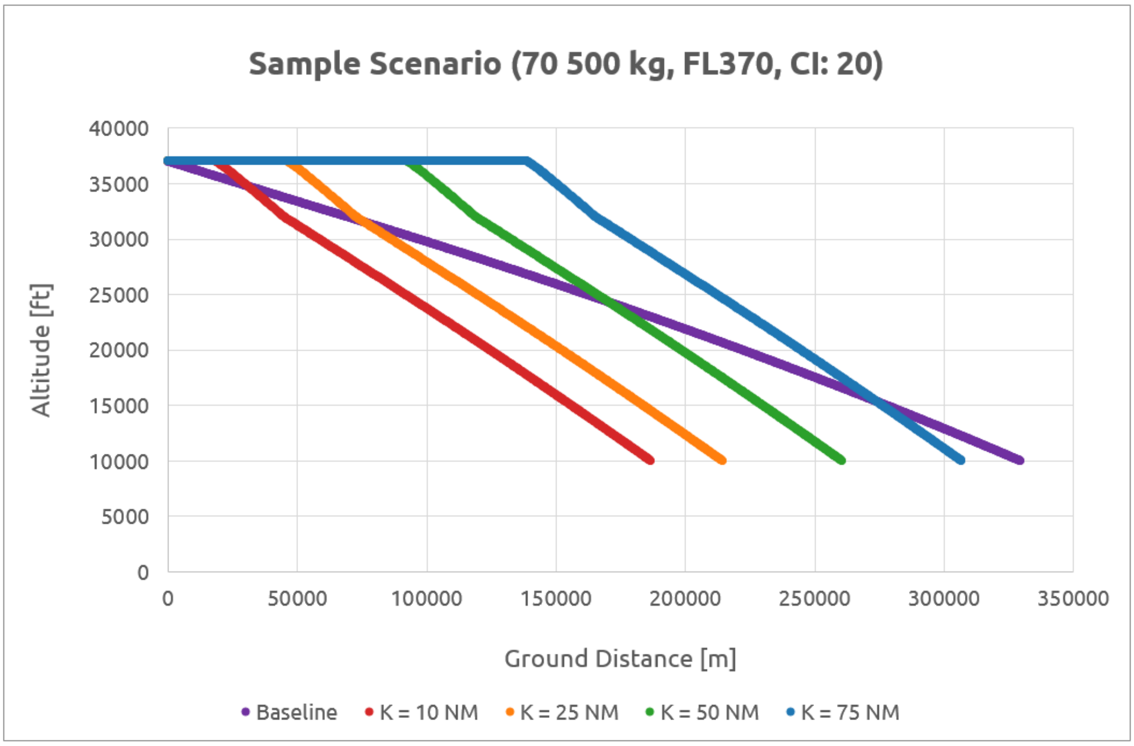

Fig. 2.1 Sample scenario plotted as ground distance vs. altitude.

2.1.2. Variables

2.1.2.1. Cruise Altitude (z)

Cruise altitude (*z*) is the altitude at which an aircraft flies its cruise phase. In this study, it corresponds to the maintained altitude at the last portion of the cruise flight phase.

It has been observed that most A320 aircraft arriving to Barcelona from the East use flight levels in the odd thousands, while most aircraft arriving from the West use flight levels in the even thousands. Since the latter case usually involves airplanes coming from the rest of Iberia and islands in the Atlantic, the distances tend to be short and hence, their maximum height is below the maximum height of flights coming from the rest of Europe. On the other hand, the best performance of the A320 is achieved in the upper airspace, closer to its certified service ceiling of 39 100 ft.

Taking these numbers and behaviors into account, four cruise altitudes are proposed: FL300, FL320, FL350 and FL370. This way, there are levels: in the even and odd thousands; relatively evenly spaced; extended across the optimal cruise heights for this aircraft; and in line with the operations at the Barcelona-El Prat Airport.

2.1.2.2. Mass (m)

The total mass (*m*) of an active aircraft combines the mass of the empty aircraft, with that of its crew, passengers and cargo; and the mass of the fuel it is carrying.

Given that the MLW for the A320-232 is either 64 500 kg or 66 000 kg; that the MTOW of such model ranges between 67 000 kg and 78 000 kg (in both cases depending on the model); and that presumably no more than 500 kg of fuel will be spent during descent and approach; the masses for this study have been determined as follows: 64 500 kg, 66 500 kg, 68 500 kg and 70 500 kg.

It is well known that airlines tend to operate in such way that the masses of their planes at landing are close to the MLW, which makes the first two values closer to real-life operations. The other two values allow the study to have a broader image of how mass interacts with the other variables.

2.1.2.3. Cost Index (CI)

The cost index (*CI*) is a value that quantifies the trade-off between operating costs per hour and incremental fuel burn [23]. It is the quotient between the cost of time and the cost of fuel (thus, a smaller cost index means that the aim is to have a smaller fuel consumption; and a larger one means that the aim is to spend the minimum time possible).

For an A320, cost index values are traditionally in the range 0-99 (depending on FMS vendor it could also be scaled as 0-999) [23]. Although the exact numbers are private information of each airline, the general consensus seems to be that normal values are between 20 and 40. Therefore, for this study the cost index values will be: 0, 20, 40 and 60.

A given cost index represents a singular optimal Mach/CAS descent setting for each particular trajectory. Hence why this study compares trajectories based on cost index and fuel consumption rather than based on time or speed magnitudes.

2.1.2.4. K Distance (k)

The main part of this study is its independent variable: the *k* distance between TOD_{VS} and TOD_{idle} (see Fig. 1.3). A larger *k* distance means that the constant-vertical-speed trajectory will meet the idle-thrust one later: therein lie the inefficiencies of early descents.

Since the model of this study requires the two trajectories to meet before reaching FL100, it is important to know how large can *k* be (*maximum k*). In order to know this, the ground distance of the baseline trajectory is compared with the ground distance of a comparative trajectory beginning at *k* = 0 (i.e., $TOD_{idle} = TOD_{VS}$) by subtracting the former from the latter. The limiting case was used: trajectories with the heaviest mass, 70 500 kg, would have the minimum maximum *k*.

Table 2.1. Possible *k* distances.

Cruise altitude (z) [-]	Cost Index (CI) [-]	Maximum k [NM]	Allows for: [NM]			
			***k* = 10**	***k* = 25**	***k* = 50**	***k* = 75**
FL300	0	38.23	Yes	Yes	-	-
FL320	0	43.75	Yes	Yes	-	-
FL300	20	49.43	Yes	Yes	-	-
FL350	0	52.75	Yes	Yes	Yes	-
FL320	20	58.45	Yes	Yes	Yes	-
FL370	0	59.51	Yes	Yes	Yes	-
FL300	40	74.60	Yes	Yes	Yes	-
FL350	20	75.27	Yes	Yes	Yes	Yes
FL370	20	87.06	Yes	Yes	Yes	Yes
FL320	40	87.06	Yes	Yes	Yes	Yes
FL300	60	97.54	Yes	Yes	Yes	Yes
FL350	40	105.27	Yes	Yes	Yes	Yes
FL320	60	108.20	Yes	Yes	Yes	Yes
FL370	40	115.86	Yes	Yes	Yes	Yes
FL350	60	122.97	Yes	Yes	Yes	Yes
FL370	60	130.70	Yes	Yes	Yes	Yes

After the values of the third column were retrieved, it was determined that the four (4) possible *k* distances of this study would be: 10 NM, 25 NM, 50 NM and 75 NM. Trajectories in which *k* couldn't reach 75 NM or 50 NM (as shown by the sixth and seventh column) were eventually eliminated from the study; reducing the number of comparative trajectories from two hundred and fifty-six (256) to two hundred and sixteen (216).

2.2. Data Retrieving and Processing

Once the model of the experiment has been defined, it is time for the data to be created, retrieved and processed. Fig. 2.2 and Fig 2.3 are a summary of the process behind this, which is further explained in the coming sections.

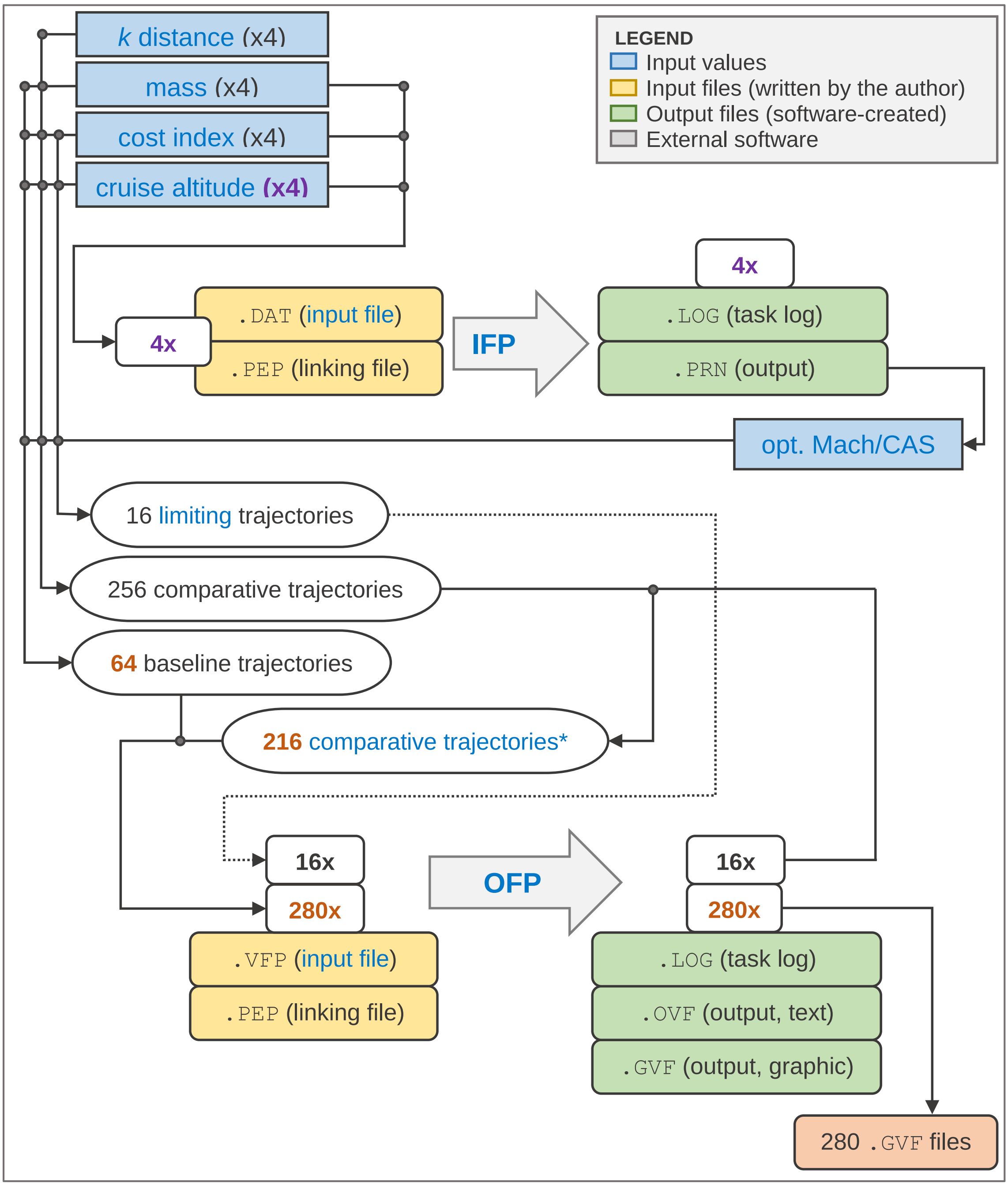

Fig. 2.2 Summary of this study's experimental methodology (part one).

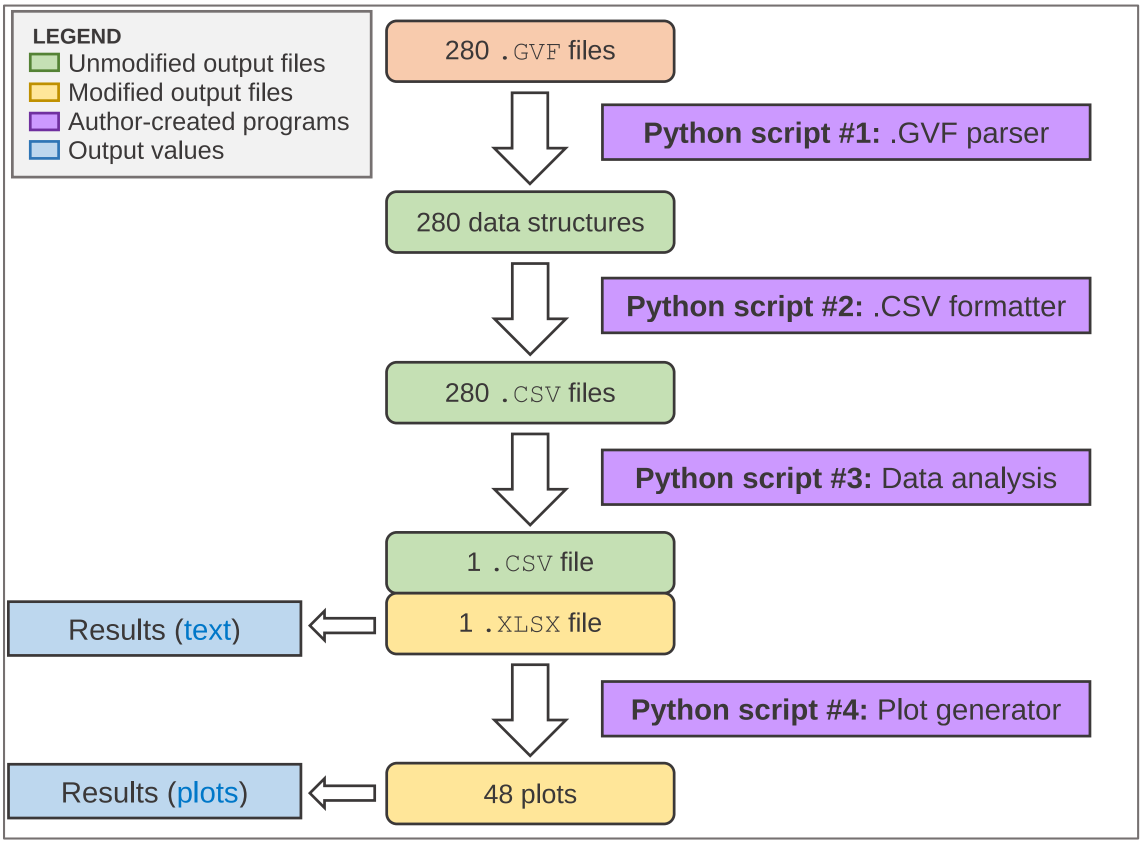

Fig. 2.3 Summary of this study's experimental methodology (part two).

2.2.1. Determination of the individual Mach/CAS settings

With the IFP PEP module (see section 1.3.), optimal descent Mach/CAS values can be determined for a given cruise altitude – mass – cost index combination. Annex A shows the input values that were used. Four .PEP sessions were created, each of them containing four files: the main .PEP linking file, a .DAT file with the input values, a .LOG file with the task log, and a .PRN file with the output. The four .PRN files were read manually to retrieve the values of Table 2.2.

Table 2.2. Determination of Mach/CAS settings for the simulations.

Cruise altitude (z) [-]	Mass (m) [kg]	Cost Index (CI) [-]	Optimal Mach/CAS [-/KCAS]
FL300	64 500	0	M 0.668 / 250.0
		20	M 0.713 / 268.1 [15]
		40	M 0.774 / 304.4
		60	M 0.793 / 340.0

[15] Even though the original file yields a slightly smaller value, 0.1 kt have been added in order to make it possible for the OFP module to reach that CAS (the value is so close to the initial Mach that the program has problems with the value's resolution and thus thinks that it has already surpassed it; comitting an error).

FL300	66 500	0	M 0.668 / 250.0
		20	M 0.714 / 268.5
		40	M 0.776 / 304.8
		60	M 0.793 / 340.0
	68 500	0	M 0.668 / 250.0
		20	M 0.715 / 268.9
		40	M 0.777 / 305.2
		60	M 0.794 / 340.0
	70 500	0	M 0.668 / 250.0
		20	M 0.716 / 269.4
		40	M 0.778 / 305.7
		60	M 0.794 / 340.0
FL320	64 500	0	M 0.696 / 250.0
		20	M 0.750 / 271.2
		40	M 0.782 / 307.5
		60	M 0.797 / 340.0
	66 500	0	M 0.696 / 250.0
		20	M 0.752 / 271.8 [16]
		40	M 0.783 / 308.0
		60	M 0.797 / 340.0
	68 500	0	M 0.696 / 250.0
		20	M 0.753 / 272.2 [16]
		40	M 0.784 / 308.4
		60	M 0.797 / 340.0
	70 500	0	M 0.696 / 250.0
		20	M 0.754 / 272.6 [16]
		40	M 0.785 / 308.9
		60	M 0.795 / 340.0
FL350	64 500	0	M 0.741 / 250.0
		20	M 0.773 / 276.0
		40	M 0.789 / 312.3
		60	M 0.795 / 340.0
	66 500	0	M 0.741 / 250.0
		20	M 0.775 / 276.4
		40	M 0.788 / 312.7
		60	M 0.792 / 340.0
	68 500	0	M 0.741 / 250.0
		20	M 0.777 / 276.9
		40	M 0.786 / 313.2
		60	M 0.790 / 340.0
	70 500	0	M 0.741 / 250.0
		20	M 0.778 / 277.3
		40	M 0.785 / 313.6
		60	M 0.787 / 340.0
FL370	64 500	0	M 0.761 / 250.0
		20	M 0.779 / 279.1
		40	M 0.785 / 315.5
		60	M 0.787 / 340.0

[16] Even though the original file yields a slightly smaller value, 0.1 kt have been added in order to make it possible for the OFP module to reach that CAS (the value is so close to the initial Mach that the program has problems with the value's resolution and thus thinks that it has already surpassed it; comitting an error).

FL370	66 500	0	M 0.764 / 250.0
		20	M 0.778 / 279.6
		40	M 0.781 / 315.9
		60	M 0.785 / 340.0
	68 500	0	M 0.766 / 250.0
		20	M 0.776 / 280.0
		40	M 0.778 / 316.4
		60	M 0.782 / 340.0
	70 500	0	M 0.767 / 250.0
		20	M 0.775 / 280.4
		40	M 0.776 / 316.7
		60	M 0.781 / 340.0

2.2.2. Simulation of the trajectories

After retrieving the Mach/CAS setting for every case, it is possible to simulate all the trajectories. A different PEP module, the OFP was used for this purpose (see section 1.3.). Two hundred and eighty (280) simulations were run: two hundred and sixteen (216) for the comparative trajectories (as established in section 2.1.2.4.); and their sixty-four (64) baseline trajectories.

Every simulation was a `.PEP` session in itself, containing five files: the main `.PEP` linking file, a `.VFP` file with the input values (Annex B shows the input values that were used), a `.LOG` file with the task log, and two output files in different formats: `.GVF` (graphic-oriented) and `.OVF` (text-oriented).

Four Python scripts were developed in order to process the data (Fig. 2.3), mainly using a data analysis tools library called *Pandas*. The first script converted the `.GVF` files into labeled data structures, while the second one formatted these as `.CSV` files. The third script calculated the *h* altitude of every baseline/comparative pairing, organized the information accordingly and output condensed results in a single `.CSV` file. Since the independent variable of the simulations' output files is time rather than ground distance, some linear interpolation had to be done when comparing trajectories. A fourth script converted that last single `.CSV` file into plots.

CHAPTER 3. Results

In this chapter, the different plots resulting from section 2.2.2. are shown. The information retrieved after analyzing those figures is available in the discussion (section 3.2.).

In any case it is important to take into account what kind of numbers we are dealing with in this chapter. Relative values were chosen for the plots because they allow for a fairer comparison between different scenarios; however, they can be slightly misleading regarding the impact of possible fuel savings in descent operations. In order to clarify the magnitude of fuel inefficiency, a few values are shown in the next table.

Table 3.1. Average absolute values of fuel consumption.

***K* distance [NM]**	**Avg. f_b [kg]**	**Avg. f_k [kg]**	**Fuel Inefficiency (Min., Avg., Max.) [kg]**	**Avg. α* [-]**
10	69.0	67.6	(-1.9, 1.4, 9.2)	1.89%
25	181.3	171.3	(-2.1, 10.0, 34.3)	5.35%
50	372.9	336.2	(7.5, 36.7, 78.8)	10.47%
75	553.5	482.1	(35.2, 71.5, 116.9)	14.66%

3.1. Plots

These plots show *k* distance (2.1.2.4.) versus extra fuel consumption in percentage (α*, as defined by Formula 2.2). In order to ease the analysis of data, three types of plots were generated: one where each plot is for a given mass and a given cost index (Fig. 3.1); another one where each plot is for a given mass and a given cruise altitude (Fig. 3.2); and one where each plot is for a given cruise altitude and a given cost index (Fig. 3.3).

3.1.1. Given mass and given cost index

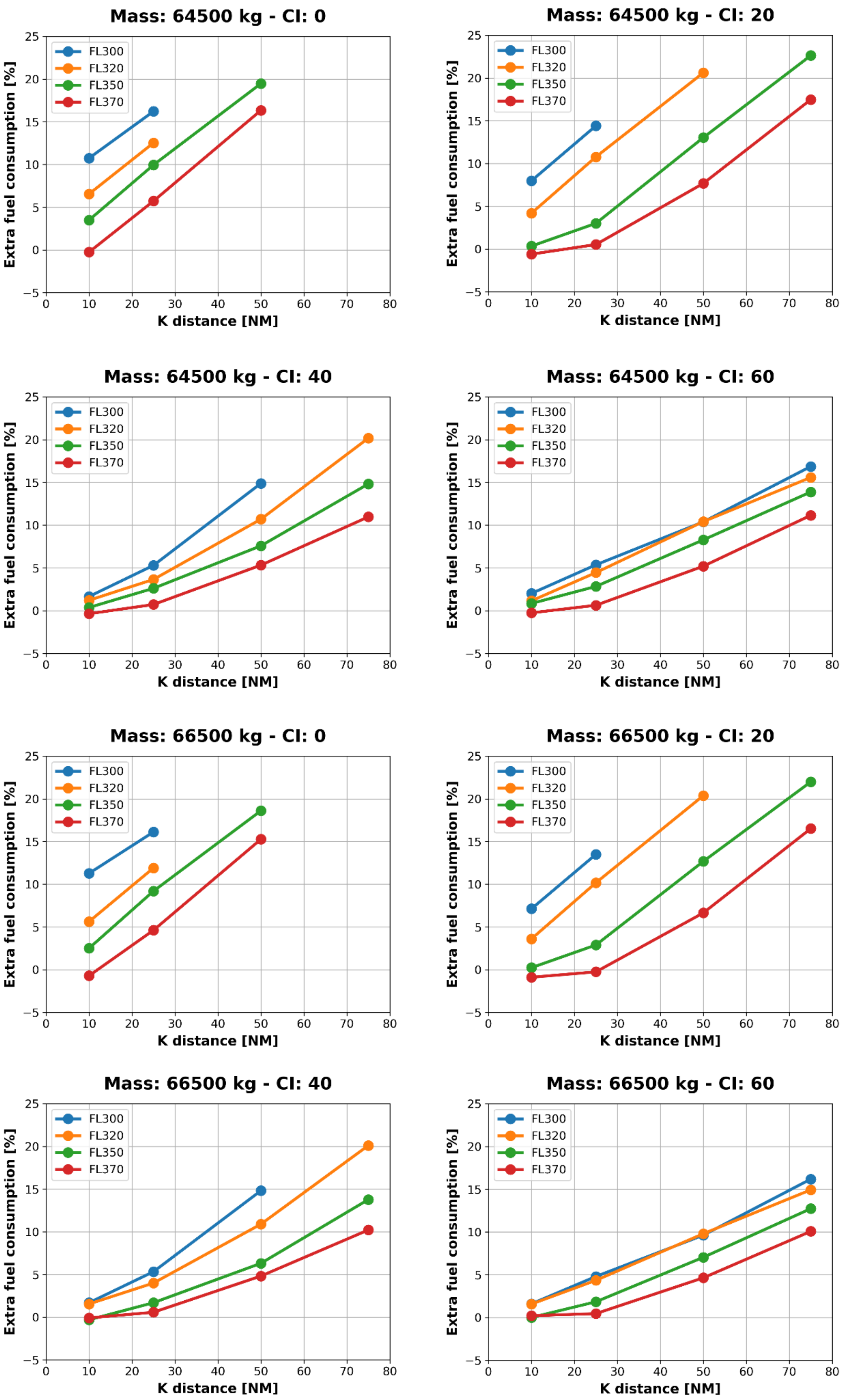

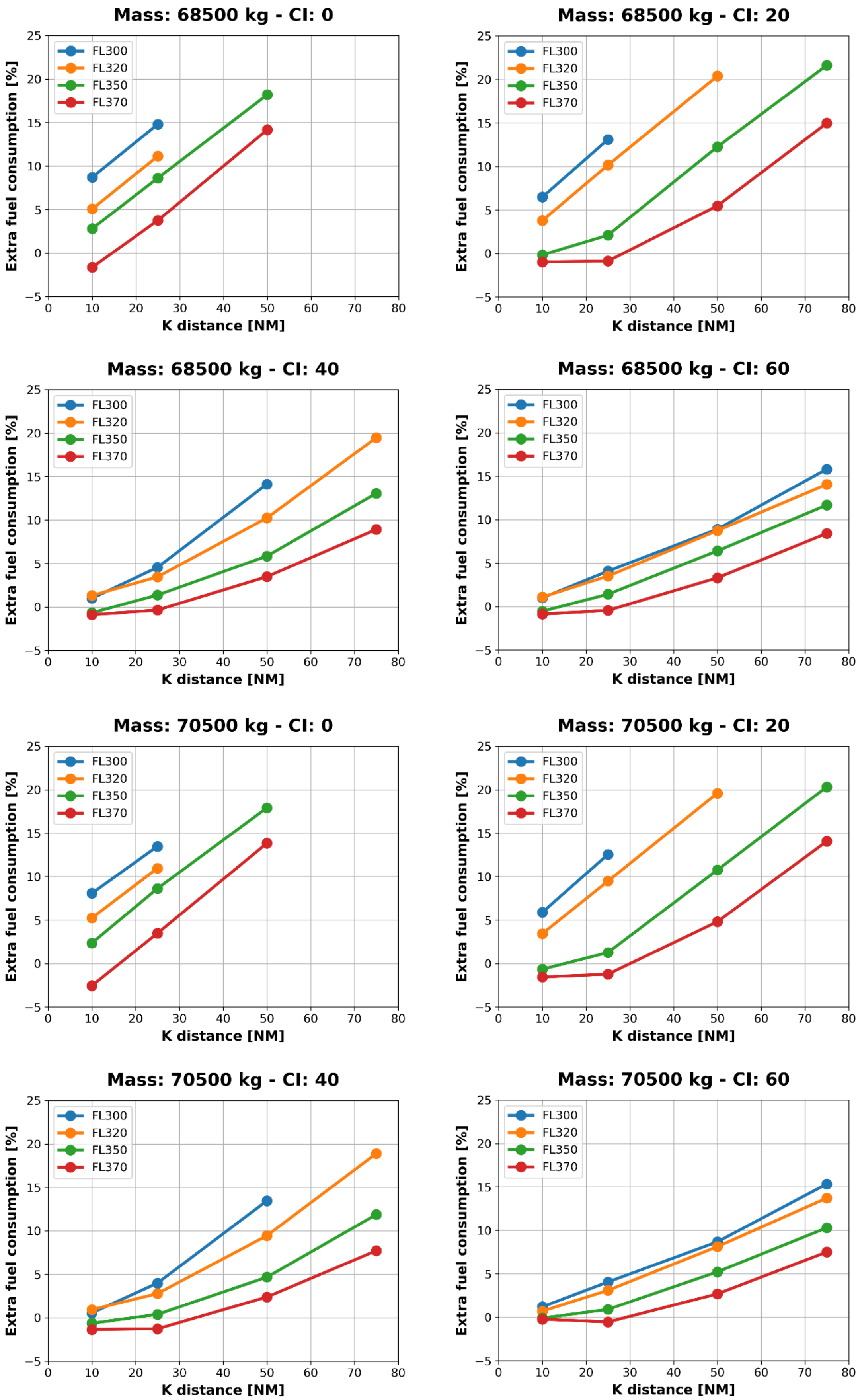

Fig. 3.1 Results by mass-cost index pairings *(grouped)*

3.1.2. Given mass and given cruise altitude

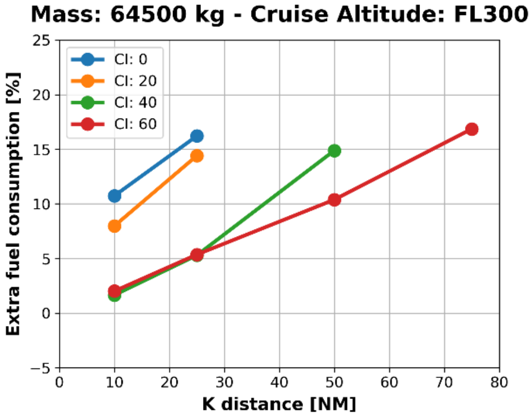

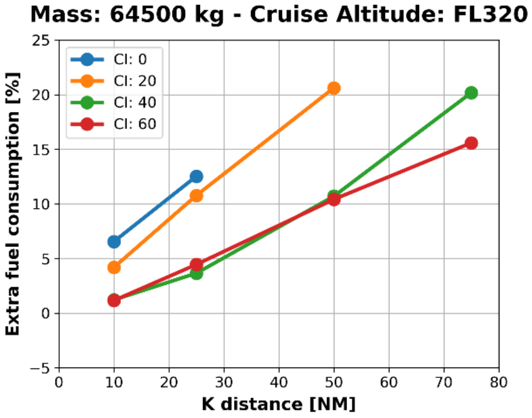

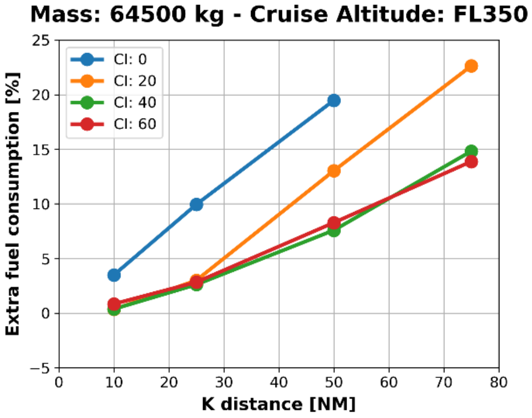

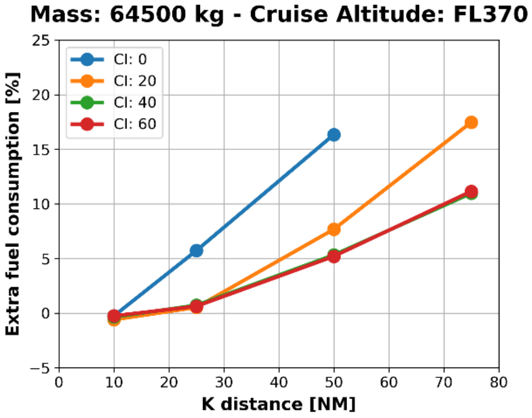

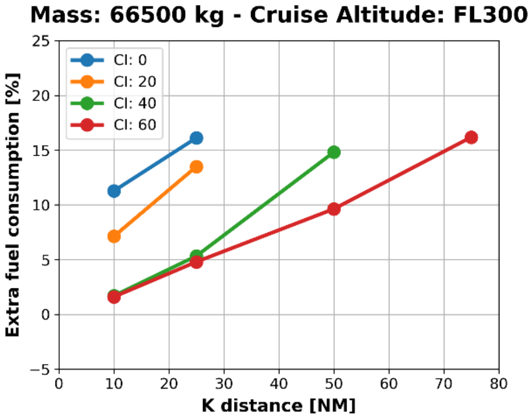

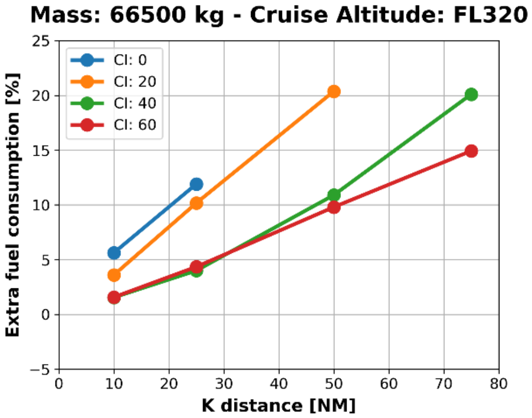

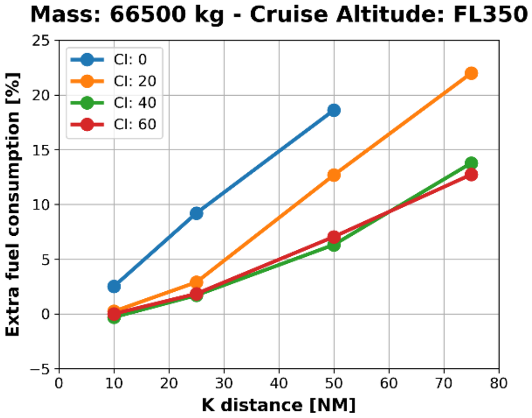

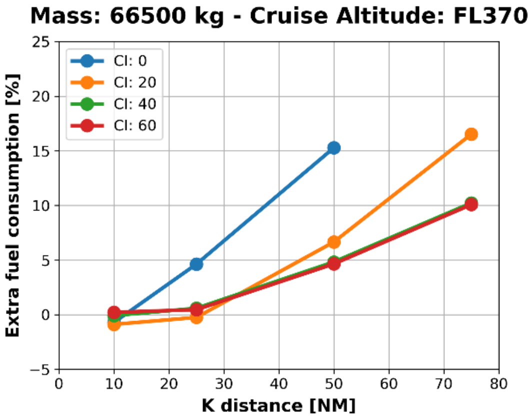

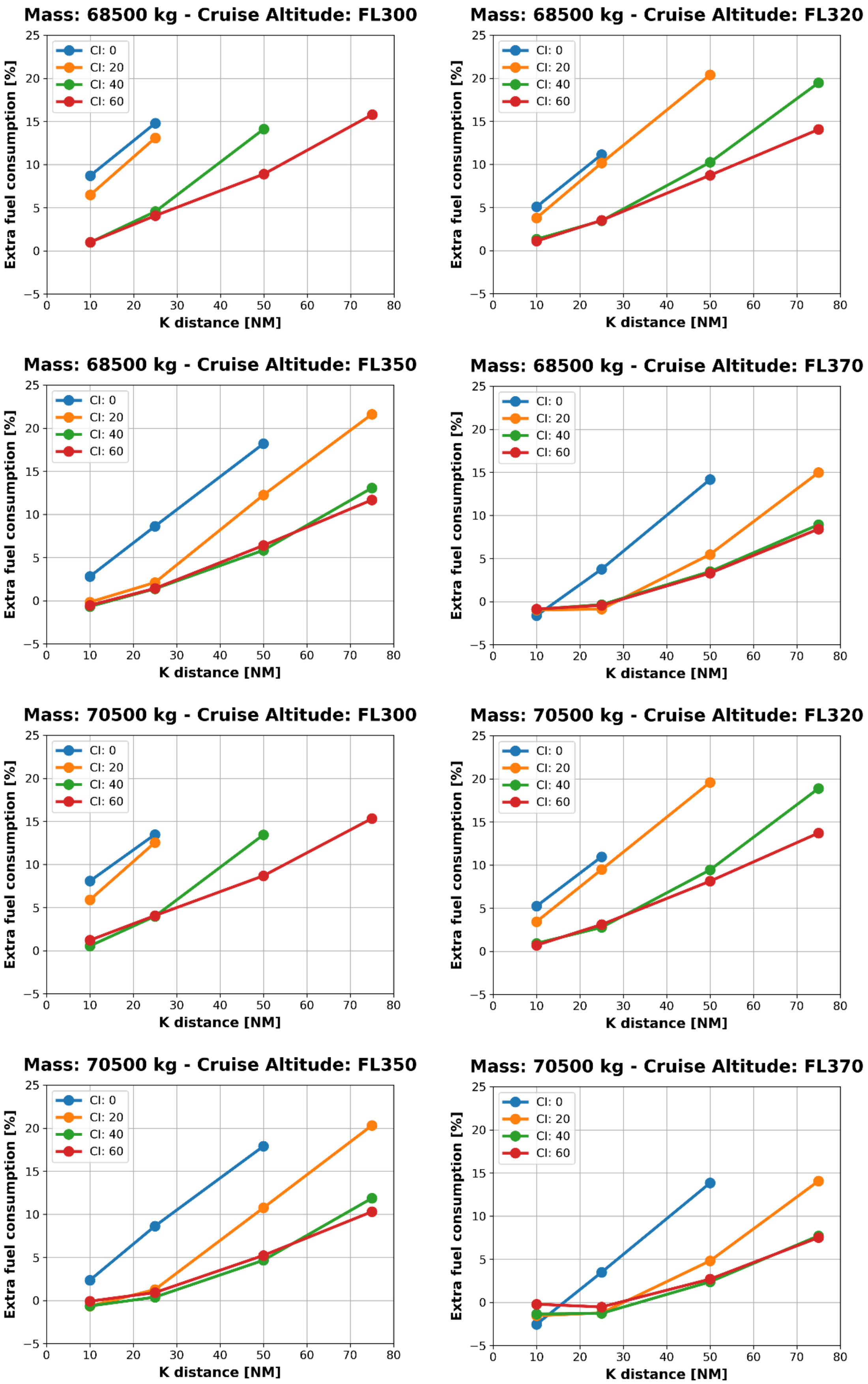

Fig. 3.2 Results by mass-cruise altitude pairings *(grouped)*

3.1.3. Given cruise altitude and given cost index

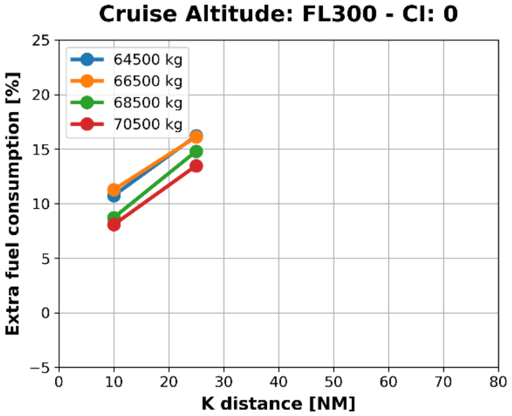

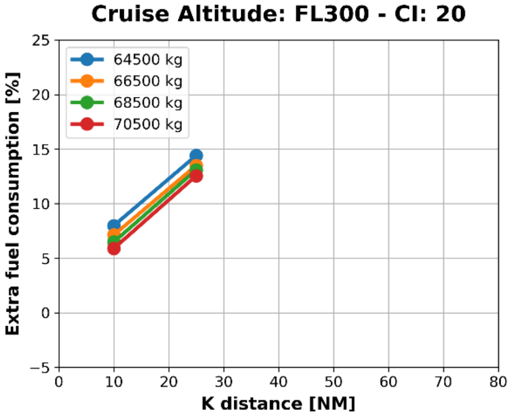

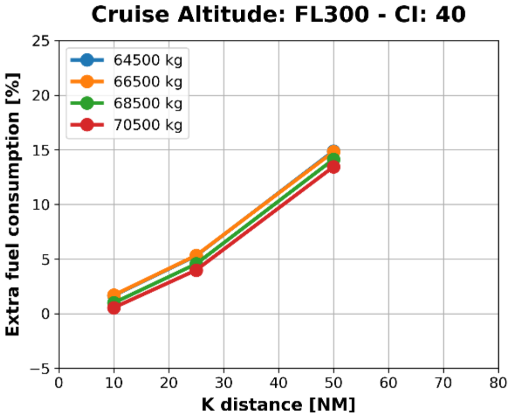

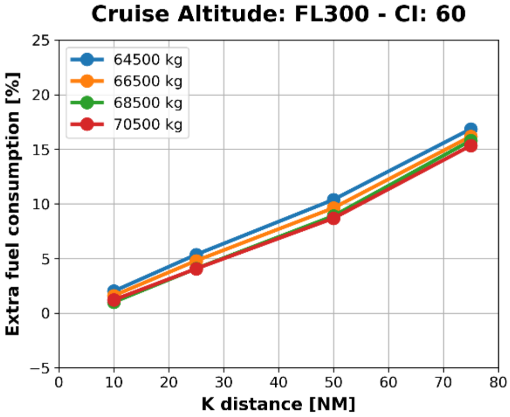

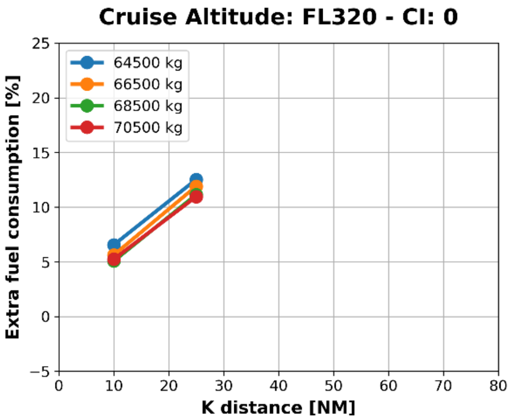

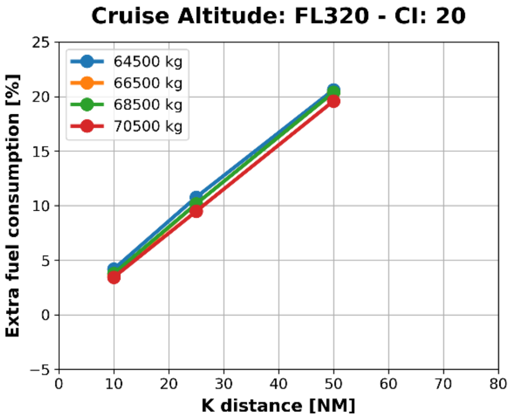

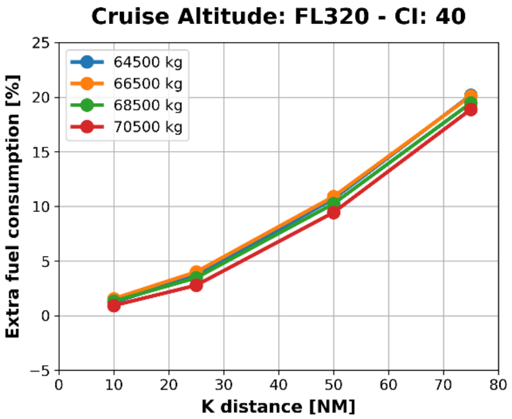

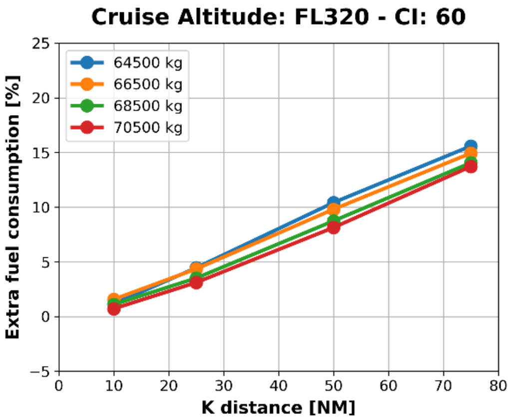

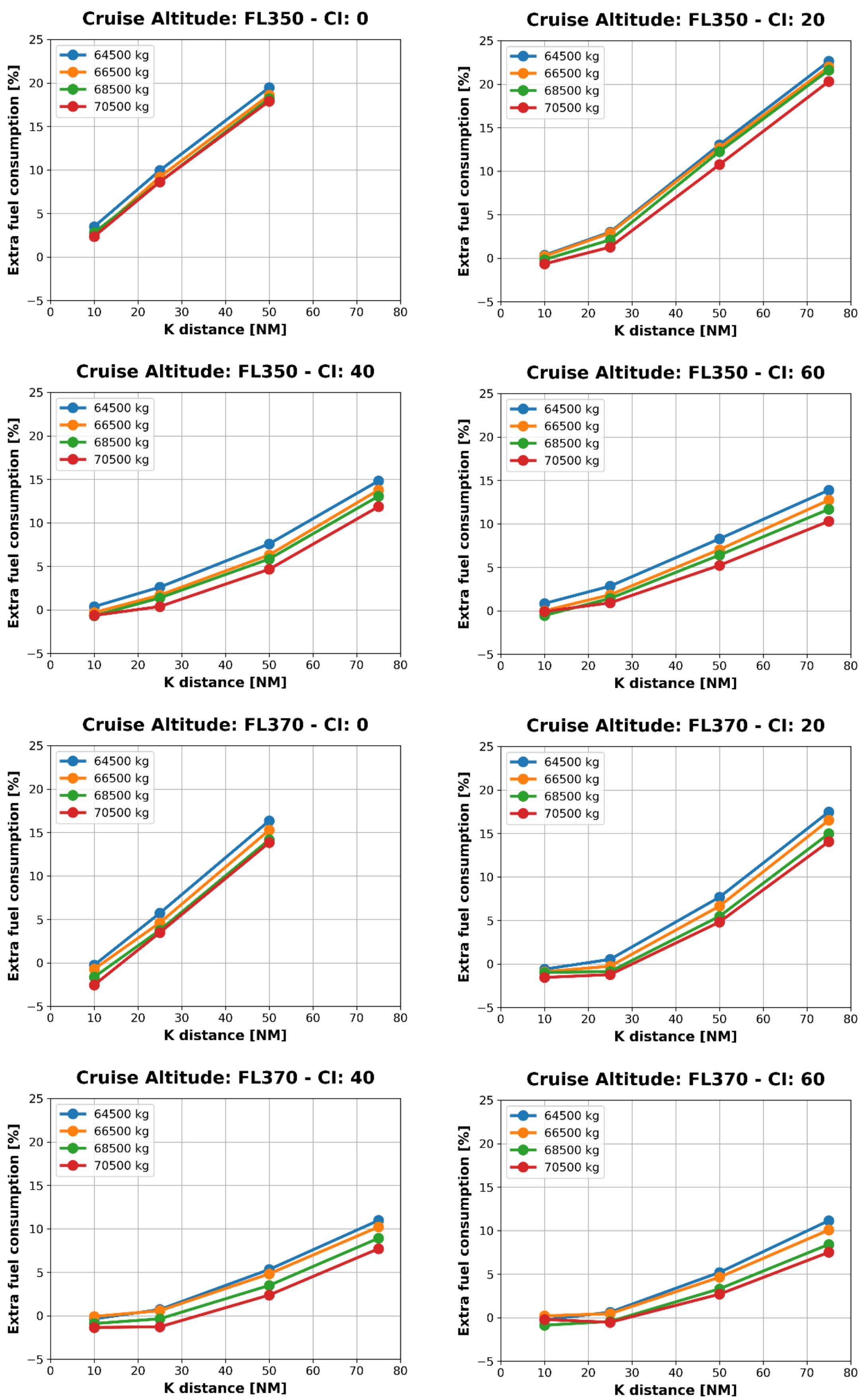

Fig. 3.3 Results by cost index-cruise altitude pairings *(grouped)*

3.2. Discussion

Retrieving and processing data from the different scenarios created by the two hundred and eighty (280) simulations, has resulted in a total of two hundred and sixteen (216) data points visible in the plots of the previous pages. As expected, most of the scenarios have yielded a positive extra fuel consumption (i.e., a fuel inefficiency), with the maximum value reaching 22.63% or 116.9 kg of fuel. Only in twenty-nine (29) cases (13.43%), there was a negative fuel inefficiency (with the smallest relative value being -2.55%, and the smallest absolute value being -2.1 kg).

According to the model of this study, an early descent (before the interception point at altitude *h*) spends fuel according to its constant-vertical-speed setting (hitherto, **pattern *b***). Whereas the descent trajectory to which it is being compared has two fuel consumption patterns: one for the cruise segment from TOD_{vs} to TOD_{idle} (**pattern *c***), and one for the idle-thrust segment from TOD_{idle} to the interception point at altitude *h* (**pattern *k***). It is fairly clear that *pattern k* is more efficient than *pattern b*, but the appearance of negative fuel inefficiencies reveals that *pattern b* is most likely more efficient than *pattern c* for some specific cases. Therefore, there is a trade-off between the consumption of *pattern b* and the fuel savings of *pattern k* combined with the extra consumption of *pattern c*. It is worth noting that all negative fuel inefficiencies are rather small, and that they were found only for very particular flight conditions, namely: *z* = FL350, FL370 and for *k* = 10 NM, 25 NM.

In general and as expected, the different trends from Fig. 3.1 show that the greater the *k* distance is, the more fuel inefficient the descent will be. It is a logical result, considering that increasing *k* means increasing the deviation from the intended optimal flight profile. It is also perceived that the relation between fuel inefficiency and cruise altitude is of one being inversely proportional to the other.

In the case of Fig. 3.2, the cost index parameter exhibits a somewhat unusual behavior: for a given mass, a given cruise altitude and a given *k* distance; an increase in cost index does not necessarily mean a decrease or increase of fuel inefficiency (especially at *k* = 10NM, 25 NM). When going from CI = 0 to CI = 20, fuel consumption varies little as compared to when going from CI = 40 to CI = 60; and this goes in line with the variation behavior of CAS values in those same cases (see Table 2.2.). Nevertheless, the MMO/VMO constraint (which directly affects the Mach/CAS optimal values for CI = 60) might be showing an inadequate picture.

Fig. 3.3 shows that mass is inversely proportional to fuel inefficiency, but variation is visibly inferior to the one caused by cruise altitude (i.e., the impact on fuel inefficiencies caused by cruise altitude is stronger than that caused by mass). All in all, the relation between *k* distance and extra fuel consumption seems to be polynomial in nature (further backed by the aforementioned appearance of negative values).

CONCLUSIONS

In spite of the perceived simplicity of the experiment conducted in this study, it has permitted the confirmation of the hypothesis that descent anticipation represents a non-trivial fuel inefficiency; and most importantly, this study has achieved a first relative quantification of such inefficiency. In a world of increasing traffic, even the smallest values of fuel savings can prove significant in the aggregate level, whether for an operator or for the whole system; and with savings of up to a fifth part in relative fuel consumption (up to 116.9 kg of absolute fuel savings[17]; see Table 3.1.), descent procedures are not to be neglected from the fuel optimization paradigm currently booming in aviation research and its vision for the future.

The realization of this first experiment has also highlighted the need for further research into this topic in order to better understand the relation between all the variables, even if a few patterns have already been identified. It is undoubtedly necessary: to attempt to extract an approximate formula of the interaction between the independent variables (this could even be done with the data used in this experiment); to consider more k values (especially between k = 0 NM and k = 25 NM); and to design a specialized experiment that deals with cost index and its relation to fuel inefficiency. It is also required to incorporate wind and temperature as variables in a future study, something overlooked in this experiment.

The present being a very generic model, it would be worthwhile to assess a real life specialized case study based on the approach used in this work; both for CDO (Continuous Descent Approach) and non-CDO (most of the current) operations; yielding actual numbers for that extra fuel spent. This could be complemented with research into the reasons behind early descents, in order to provide both airspace users and the ATC (Air Traffic Control) system with new ideas that might influence their decision making when flight planning and managing for this flight phase.

Pure CDO operations might be far from the general standard in the near future, but the ongoing advances in all sorts of aviation resources will make flight profiles increasingly flexible (versus the contemporaneous profiles) over time; and thus, profiles will be growingly closer to the ideal efficient descent path. *How close* will depend on the decisions taken, and the available information behind them.

[17] Such savings would represent, per descent, spending $87.11 less and emitting 368.2 kg of CO_2 less. These values are calculated assuming jet fuel price as $2.2680/gal or $0.7452/kg (taking Jet A-1's density as 0.804 kg/l; and the global average of jet fuel price as of 19 October 2018 [24]); and assuming 3.15 kg of CO_2 emissions per kg of Jet A-1 fuel [25].

BIBLIOGRAPHY AND REFERENCES

[1] Clarke, J-P., Ho N. T., Ren L. et al. “Continuous Descent Approach: Design and Flight Test for Louisville International Airport”. *Journal of Aircraft.* Vol. 41, No. 5, September-October (2004), pp. 1054-1066. DOI: 10.2514/1.5572.

[2] Park, S. G. and Clarke, J-P., “Optimal Control Based Vertical Trajectory Determination for Continuous Descent Arrival Procedures”. *Journal of Aircraft*. Vol. 52, No. 5 (2015), pp. 1469-1480. DOI: 10.2514/1.C032967.

[3] Dalmau, R. and Prats, X., “Controlled time of arrival windows for already initiated energy-neutral continuous descent operations”. *Transportation Research Part C: Emerging Technologies.* Vol. 85 (2017), pp. 334-347. DOI: 10.1016/j.trc.2017.09.024.

[4] Airbus, *Orders and Deliveries – September 2018 – Commercial Aircraft*. Excel file (ODs-Airbus-Commercial-Aircraft-September-2018.xlsx), data available until 30 September (2018). Downloaded 17 October 2018 from: https://www.airbus.com/aircraft/market/orders-deliveries.html

[5] Airbus. *A320ceo* website. Retrieved 18 October (2018) from: https://www.airbus.com/aircraft/passenger-aircraft/a320-family/a320ceo.html

[6] Airbus, “EFW secures launch contract for A321P2F”. *Newsroom Press Releases*. Published 07 February (2018). Retrieved 04 August 2018 from: https://www.airbus.com/newsroom/press-releases/en/2018/02/efw-secures-launch-contract-for-a321p2f-conversion-from-vallair-.html

[7] Flight Ascend Consultancy, *Global Aviation Sector Overview.* Published 21 February (2017). Slide 15 (Flight Fleet Forecast). Retrieved 04 August 2018 from: http://www.aviationnews-online.com/wp-content/video/Korea-2017/slides/d2-02.pdf

[8] CAST/ICAO Common Taxonomy Team (CICCT), *Glossary*. Release 1.0. Retrieved 04 August 2018 from: http://www.intlaviationstandards.org/

[9] European Aviation Safety Agency (EASA), *EASA type rating and licence endorsement list flight crew – all aircraft excluding helicopters.* Published 12 July (2018). Retrieved 04 August 2018 from: https://www.easa.europa.eu/sites/default/files/dfu/20180712%20EASA%20T_R_List_Acft.pdf

[10] Plane-spotter.com, *Deciphering the AIRBUS codes.* Published 12 October (2006). Retrieved 04 August 2018 from: http://bgspotters.net/LBSF/Deciphering_the_Airbus_codes1.pdf

[11] Centre for Aviation (CAPA), *Barcelona El Prat: Europe's leading airport for LCCs a battleground in fight for business travelers.* Published 01 July (2015). Retrieved 16 October 2018 from: https://centreforaviation.com/analysis/reports/barcelona-el-prat-europes-leading-airport-for-lccs-a-battleground-in-fight-for-business-travellers-232840

[12] European Aviation Safety Agency (EASA), *EASA Type-Certificate Data Sheet No. EASA.A.064 for AIRBUS A318-A319-A320-A321*. Issue No. 16. Published 06 March (2015). Retrieved 04 August 2018 from: https://www.easa.europa.eu/sites/default/files/dfu/TCDS_EASA%20A%20064_%20Airbus_%20A318_A319_A320_A321_Iss16_20150306.pdf

[13] International Air Transport Association (IATA), *Loss of Control In-Flight Accident Analysis Report.* International Air Transport Association, Montréal/Geneva (2015), p. 31. ISBN: 978-92-9252-775-4.

[14] Airbus, *A319/A320/A321 Flight Crew Operating Manual (FCOM)*. Rev. 36 (2003), Vol. 1 (Systems Description); 1.22.30 (pp. 2, 25, 27). Version for CCM Airlines.

[15] Smart Cockpit, *Airbus Descent Monitoring*. V1.1, June (2007). Retrieved 18 October 2018 from: http://www.smartcockpit.com/docs/Airbus_Descent_Monitoring_1.pdf

[16] Airbus, *A319/A320/A321 Flight Crew Operating Manual (FCOM)*. Rev. 36 (2003), Vol. 4 (FMGS Pilot's Guide); 4.05.60 (pp. 2-6). Version for CCM Airlines.

[17] Verdonk Gallego, C. E., Gómez Comendador V. F., Sáez Nieto, F. J., Orenga Imaz, G., Arnaldo Valdés R. M., "Analysis of air traffic control operational impact on aircraft vertical profiles supported by machine learning". *Transportation Research Part C: Emerging Technologies.* Vol. 95 (2018), pp. 883-903. DOI: 10.1016/j.trc.2018.03.017.

[18] René van Paassen, M. M., Coelho P. N. P., Mulder, M., "Support Interface for Continuous Descent Approaches". *IFAC Proceedings Volumes*. Vol. 34, No. 16 (2001), pp. 199-204. DOI: 10.1016/S1474-6670(17)41525-4.

[19] Corker K. M., Pisanich G. M., "Analysis and Modeling of Flight Crew Performance in Automated Air Traffic Management Systems". *IFAC Proceedings Volumes*. Vol. 28, No. 15 (1995), pp. 547-552. DOI: 10.1016/S1474-6670(17)45289-X.

[20] Spinardi, G., "Up in the air: Barriers to greener air traffic control and infrastructure lock-in in a complex socio-technical system". *Energy Research & Social Science.* Vol. 6 (2015), p. 41-49. DOI: 10.1016/j.erss.2014.11.006.

[21] Airbus, *Performance Programs Manual (PPM)*. Rev. 02. Chapters 10, 40, 50. Published 01 August (2007). Retrieved 18 July 2018 from: http://122.166.54.52/AIPEP/start.htm

[22] Rodrigues de Lemos, J. P., *Takeoff and Landing Performance Optimization: Development of a Computational Methodology.* Published October (2011). Instituto Superior Técnico, Lisbon. Retrieved 12 July 2018 from: https://fenix.tecnico.ulisboa.pt/downloadFile/395143164279/Jo%C3%A3o%20Lemos%20Viana%20-%20Takeoff%20and%20Landing%20Performance%20Optimization.pdf

[23] Airbus Customer Services, *Getting to grips with the cost index.* Published May (1998). No. 2., pp. 5-8. Retrieved 17 October 2018 from: http://ansperformance.eu/references/library/airbus-cost-index.pdf

[24] International Air Transport Association (IATA). Jet Fuel Price Monitor webpage. Retrieved 22 October 2018 from: https://www.iata.org/publications/economics/fuel-monitor/Pages/index.aspx

[25] International Air Transport Association (IATA). *IATA Carbon Offset Program – FAQ Airline Participants.* Version 10.0, p. 8. Published 19 January (2016). Retrieved 22 October 2016 from: https://www.iata.org/whatwedo/environment/PublishingImages/ICOP%20FAQ%20general%20for%20airline%20participants%20jan%202016.pdf

APPENDIX A. Input values for the IFP module.

Aircraft
Type: A320
Model: A320-232
Characteristics: V2527-A5 - Fadec SCN 17
Option: Standard with FMS1 speeds

Phase
Phase: Descent
Type: Integrated
Option: Descent at given cost index

Aerodynamic data
Configuration: CLEAN
Center of gravity location (%): 25.0
Drag factor: 1.000

Engine data
Engine level: Average
Thrust:
- Rating: Idle

Bleeds selections:
- Air conditioning: NORM
- Anti ice: Off

Atmospheric data
Temperature: ISA deviation (Celsius)
Wind: Analytical
- Wind at sea level (kt): 0
- Wind gradient (kt/1000ft): 0.0

Calculation data
Parameter: Initial weight (kg)
- Input mode: Increasing list
  - First: 64500
  - Step: 2000
  - Last: 70500

Parameter: Cost index (kg/min)
- Input mode: Increasing list
  - First: 0
  - Step: 25
  - Last: 75

Descent profile:
- Speed limitation altitude: 10000 ft
- Speed limitation CAS: 250 kt
- Initial altitude: z (Possible values: 30000, 32000, 35000, 37000)
- Final altitude: 10000 ft

APPENDIX B. Input values for the OFP module.

Aircraft
Type: A320
Model: A320-232
Characteristics: V2527-A5 – SEPCARB III Carbon brakes 70 MJ +BSCU Std9 + SCN 17
Version: 01

Computation Type: From any point in flight

Initial conditions
Aircraft limitation:
- CG option: Basic
- Max pitch attitude during flight (°): 30

Bleeds selection:
- Air conditioning: Normal
- Anti ice: Off

Initial data:
- Configuration: CONF 0
- Speed type: Mach
- Altitude type: Pressure altitude
- Direction type: True course
- Flight parameters and values:
    - Weight (kg): m (Possible values: 64500, 66500, 68500, 70500)
    - CG location (%): 25
    - Altitude (ft): z (Possible values: 30000, 32000, 35000, 37000)
    - Mach: Mach
    - Time (s): 0
    - X Distance (m): 0
    - Y Distance (m): 0
    - Bank angle (°): 0
    - Direction value (°): 0
- Initial point at constant speed: Yes

Landing gear: Up
Engine(s) out: 0
Engine:
- Engine level: Average
- Thrust rating: Adapted thrust
- Adapted thrust type: Rate of climb all engines
- Value (ft/mn): 0

Atmospheric
Temperature:
- Temperature option: ISA deviation
    - -5000 ft: 0 °C
    - 0 ft: 0°C
    - 36089 ft: 0°C
    - 50000 ft: 0°C

Humidity:
- Relative humidity option: Standard

Wind:
- -5000 ft: 0 kt, 0°
- 50000 ft: 0 kt, 0°

Flight segment
(*Depending on whether this is a baseline or a comparative trajectory, the input values are different. The following pages show both cases*).

================= Flight segments (for the baseline trajectories) =================

- Segment number 1
  - Description: MACH CONSTANT SEGMENT
  - Configuration or gear transition: None
  - Engine:
    - Thrust rating: Adapted thrust
    - Engine(s) out: 0
    - Adapted thrust type: Rate of climb all engines
    - Value (ft/mn): -1000
  - Skip segment: No
  - Flight segment description:
    - Segment type: Constant speed
    - Speed type: Mach
  - Segment end:
    - Type: One end condition
    - (1) End of segment name, value: Speed CAS (kt), CAS
  - Bleeds selection:
    - Air conditioning: Normal
    - Anti ice: Off
- Segment number 2
  - Description: CAS CONSTANT SEGMENT (1)
  - Configuration or gear transition: None
  - Engine:
    - Thrust rating: Adapted thrust
    - Engine(s) out: 0
    - Adapted thrust type: Rate of climb all engines
    - Value (ft/mn): -1000
  - Skip segment: No
  - Flight segment description:
    - Segment type: Constant speed
    - Speed type: CAS
  - Segment end:
    - Type: One of two conditions encountered
    - (1) End of segment name, value: Height (ft), 10000
    - (1) End of segment name, value: Relative time (s), 999[1]
  - Bleeds selection:
    - Air conditioning: Normal
    - Anti ice: Off
- Segment number 3
  - Description: CAS CONSTANT SEGMENT (2)
  - Configuration or gear transition: None
  - Engine:
    - Thrust rating: Adapted thrust
    - Engine(s) out: 0
    - Adapted thrust type: Rate of climb all engines
    - Value (ft/mn): -1000
  - Skip segment: No
  - Flight segment description:
    - Segment type: Constant speed
    - Speed type: CAS
  - Segment end:
    - Type: One of two conditions encountered
    - (1) End of segment name, value: Height (ft), 10000
    - (2) End of segment name, value: Relative time (s), 999[1]
  - Bleeds selection:
    - Air conditioning: Normal
    - Anti ice: Off

[1] *Segments in OFP cannot be longer than 1000 steps (one step = one second).*

================ Flight segments (for the comparative trajectories) ================

Segment number 1

- Description: K-DISTANCE CRUISE
- Configuration or gear transition: None
- Engine:
  - Thrust rating: Adapted thrust
  - Engine(s) out: 0
  - Adapted thrust type: Rate of climb all engines
  - Value (ft/mn): 0
- Skip segment: No
- Flight segment description:
  - Segment type: Constant speed
  - Speed type: Mach
- Segment end:
  - Type: One end condition
  - (1) End of segment name, value: Distance X (m), k
- Bleeds selection:
  - Air conditioning: Normal
  - Anti ice: Off

Segment number 2

- Description: MACH CONSTANT SEGMENT
- Configuration or gear transition: None
- Engine:
  - Thrust rating: Idle
  - Engine(s) out: 0
- Skip segment: No
- Flight segment description:
  - Segment type: Constant speed
  - Speed type: Mach
- Segment end:
  - Type: One end condition
  - (1) End of segment name, value: Speed CAS (kt), CAS
- Bleeds selection:
  - Air conditioning: Normal
  - Anti ice: Off

Segment number 3

- Description: CAS CONSTANT SEGMENT (1)
- Configuration or gear transition: None
- Engine:
  - Thrust rating: Idle
  - Engine(s) out: 0
- Skip segment: No
- Flight segment description:
  - Segment type: Constant speed
  - Speed type: CAS
- Segment end:
  - Type: One of two conditions encountered
  - (1) End of segment name, value: Height (ft), 10000
  - (2) End of segment name, value: Relative time (s), 999[2]
- Bleeds selection:
  - Air conditioning: Normal
  - Anti ice: Off

Segment number 4

- Description: CAS CONSTANT SEGMENT (2)
- Configuration or gear transition: None
- Engine:
  - Thrust rating: Idle
  - Engine(s) out: 0
- Skip segment: No

[continues in the next page]

Flight segment description:

- Segment type: Constant speed
- Speed type: CAS

Segment end:

- Type: One of two conditions encountered
- (1) End of segment name, value: Height (ft), 10000
- (2) End of segment name, value: Relative time (s), 999[2]

Bleeds selection:

- Air conditioning: Normal
- Anti ice: Off

[2] *Segments in OFP cannot be longer than 1000 steps (one step = one second).*